The Higgs boson with the ATLAS experiment at the LHC: Discovery, measurement, and searches for new physics

A DISSERTATION PRESENTED
BY
TOMO LAZOVICH
TO
THE DEPARTMENT OF PHYSICS

IN PARTIAL FULFILLMENT OF THE REQUIREMENTS
FOR THE DEGREE OF
DOCTOR OF PHILOSOPHY
IN THE SUBJECT OF
PHYSICS

HARVARD UNIVERSITY
CAMBRIDGE, MASSACHUSETTS
MAY 2016

Thesis advisor: Professor Joao Guimaraes da Costa and Melissa Franklin Tomo Lazovich

The Higgs boson with the ATLAS experiment at the LHC: Discovery, measurement, and searches for new physics

Abstract

We measured things. And searched for other things. Here is what we found, please let me graduate.

Contents

Listing of figures

Listing of tables

This is the dedication.

Acknowledgments

LOREM IPSUM DOLOR SIT AMET, consectetuer adipiscing elit. Morbi commodo, ipsum sed pharetra gravida, orci magna rhoncus neque, id pulvinar odio lorem non turpis. Nullam sit amet enim. Suspendisse id velit vitae ligula volutpat condimentum. Aliquam erat volutpat. Sed quis velit. Nulla facilisi. Nulla libero. Vivamus pharetra posuere sapien. Nam consectetuer. Sed aliquam, nunc eget euismod ullamcorper, lectus nunc ullamcorper orci, fermentum bibendum enim nibh eget ipsum. Donec porttitor ligula eu dolor. Maecenas vitae nulla consequat libero cursus venenatis. Nam magna enim, accumsan eu, blandit sed, blandit a, eros.

0

Introduction

Part I

Preliminaries

1

The Standard Model and beyond: a theoretical overview

This is some random quote to start off the chapter.

Firstname lastname

2

The ATLAS detector and the Large Hadron Collider

2.1 The Large Hadron Collider

2.2 The ATLAS Detector

Part II

Observation and measurement of Higgs boson decays to $WW*$ with the ATLAS detector in LHC Run 1 at $\sqrt{s} = 7$ and 8 TeV

Basic research is what I am doing when I don't know what I am doing.

Wernher von Braun

3

$H \to WW^* \to \ell\nu\ell\nu$ Analysis Strategy

3.1 Introduction

This chapter will present an overview of the strategy for searching for a Higgs boson in the $H \to WW^* \to \ell\nu\ell\nu$ decay topology. Its purpose is to present in broad terms how the search and measurement are undertaken, before going into details on the specific sub-categories within the broader analysis.

First, the topology of the signal final state and corresponding backgrounds are presented. Next, an overview of the variables used to reduce the backgrounds and enhance the signal is given. These will be described in general, while specific values of selection cuts and background estimation will be provided in subsequent chapters. Finally, the parameters of interest in the search and measurement will be defined, and a brief overview of the statistical treatment of the final Higgs candidates is shown.

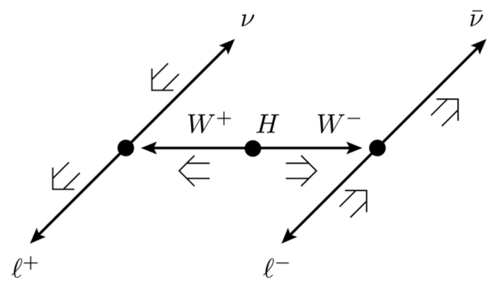

Figure 3.1: A cartoon of the WW final state. Momenta are represented with thin arrows, spins with thick arrows.[1]

3.2 Signal topology

The analysis presented here and in subsequent chapters is the study of the Higgs boson in the WW final state, where each W boson subsequently decays into a charged lepton and a neutrino. In its simplest form, the final state will then consist of two neutrinos and two charged leptons, each of which can be either an electron or a muon. If one or both of the Ws decay to τ leptons, only leptonic decays of the τ are considered, leading to additional neutrinos in the final state but still giving two charged leptons as before. Neutrinos are not detected in ATLAS, so the final state ultimately consists of two reconstructed leptons and missing transverse momentum (denoted as $E_{\mathrm{T}}^{\mathrm{miss}}$). Final states where both of the charged leptons are electrons or muons are referred to as the "same flavor" final states, while those with one electron and one muon are referred to as "different flavor".

The final state leptons will also exhibit unique correlations due to the fact that they are arising from the decay of a spin zero resonance. In particular, the spins of the final state leptons and neutrinos must all cancel, as shown in figure 3.1. Because the neutrino has a left handed helicity and the anti-neutrino has a right handed helicity, the spin and momentum of the particles will be anti-aligned and aligned, respectively. In the transverse plane, the momenta of all four final state objects must cancel as well. With the constraint of having both the momenta and the spin alignments cancel, the final state kinematics strongly prefer having a small angle between the leptons in the transverse plane (low $\Delta\phi_{\ell\ell}$). This angular correlation will also lead to low values of the di-lepton invariant mass $m_{\ell\ell}$. These unique signal final state kinematic correlations will be exploited to define the ultimate signal region.

While the basic final state consists of two leptons and $E_{\mathrm{T}}^{\mathrm{miss}}$, there can be additional objects as well depending on the production mode of the Higgs. As described in detail in Chapter 1, if the Higgs is produced via vector boson fusion production, there will be two additional forward jets in the event. Even in gluon fusion, one or more jets can be produced through initial state radiation from the incoming gluons. The analysis is separated into different signal regions depending on the number of hard jets reconstructed in the final state as well.

3.3 Background processes

Many processes from the Standard Model can also produce a final state with two leptons and missing transverse momentum . This section lists the dominant backgrounds to Higgs production. It gives general descriptions of how the backgrounds mimic Higgs production and how they can be reduced. The details of background estimation and specific cuts are left for later sections. Table3.1 summarizes the different processes.

3.3.1 Standard Model WW production

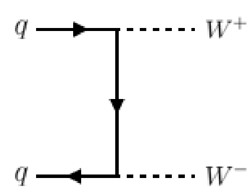

Figure 3.2: Feynman diagram for Standard Model WW production

Non-resonant Standard Model diboson production, as shown in figure 3.2, is an irreducible background to Higgs boson production in the WW final state. It produces the same exact final state objects, namely leptonically decaying W bosons. There are no additional objects in the final state that allow for background reduction. Therefore the analysis solely relies on the correlations between the leptons to reduce this background.

3.3.2 Top quark production

Production of top quarks, either in pairs ($t\bar{t}$ production) or singly (e.g. Wt production), can also mimic Higgs production. Because top quarks decay via $t \to Wb$, top pair production can produce a final state with two W bosons that then decay leptonically. In this case, however, there are two additional jets from the bottom quarks in the final state. This allows the analysis to veto on the presence of jets identified as originating from a b in order to reduce the size of the background.

Single top production can occur via s-channel, t-channel, or associated production (Wt). The mode which most closely resembles the Higgs final state is Wt. In this case, there are two real W bosons produced, as with $t\bar{t}$. However, the decay of the single top quark will still also produce one b-jet, meaning a b veto will reduce this background as well.

Figure 3.3 shows the Feynman diagrams for $t\bar{t}$ and Wt production.

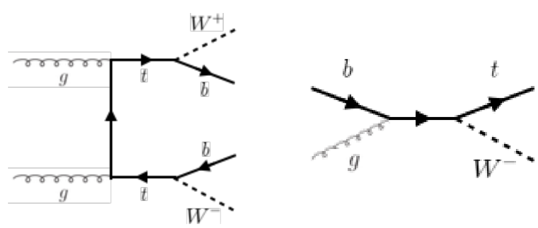

Figure 3.3: Feynman diagrams for top pair production (left) and Wt production (right)

3.3.3 W+jets background

Single W boson production, in association with jets, is a unique background. The other background considered so far have all included real leptons in the final state. In this case, however, only one real lepton from the decay of a W exists in the final state. The second reconstructed lepton can arise from two different cases. First, the lepton may truly be an algorithm “fake”, or a jet misidentified as a lepton by either the electron or muon reconstruction algorithms. Second, the lepton may be a real lepton but coming from semi-leptonic decays of particles inside the shower of the jet. This background can be reduced by requiring that the reconstructed lepton have little activity surrounding it in the calorimeter (also known as an “isolated” lepton). Figure 3.4 shows the Feynman diagram for W+jets production.

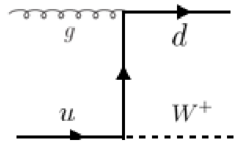

Figure 3.4: An example Feynman diagram of W+jets production

3.3.4 Z/γ^*+jets background

Production of a Z/γ^* in association with jets (also known as Drell-Yan) is also a background to Higgs production. In particular, the same flavor final states have a large Z+jets background, as the Z decays into two leptons of the same flavor. (This background also enters the different flavor final state through the leptonic decays of $Z \to \tau\tau$). Figure 3.5 shows the production of a Z in association with one jet. Because there are no neutrinos in this final state, variables like $E_{\mathrm{T}}^{\mathrm{miss}}$ can be used to reduce the background.

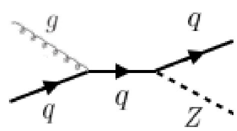

Figure 3.5: An example Feynman diagram of Z+jets production

3.3.5 Other (subdominant) backgrounds

THere are additional processes which contrinute to the background composition but are not produced as frequently as those listed already. The first of these are referred to as VV or "Other diboson" processes and include multiple Standard Model diboson processes, including WZ, ZZ, $W\gamma$, $W\gamma^*$, and $Z\gamma$ production. Additionally, there is background from QCD multijet production, where two jets are misidentified as leptons.

3.4 Isolating an $H \to WW^* \to \ell\nu\ell\nu$ signal

As presented in section 3.2, there are many different combinations of objects that can define a $H \to WW^* \to \ell\nu\ell\nu$ final state. The multiplicity of jets and the flavor combinations of the leptons both lead to a combinatorically large number of potential signal regions. Additionally, signal regions can be optimized separately to be sensitive to the distinct production modes of the Higgs. Gluon fusion, vector

Category	Process	Description
SM WW	$WW \to \ell\nu\ell\nu$	Real leptons and neutrinos
Top quark production	$t\bar{t} \to WbW\bar{b} \to \ell\nu b\ell\nu\bar{b}$	Real leptons, untagged bs
	$tW \to WbW \to \ell\nu\ell\nu b$	Real leptons, untagged b
	$t\bar{b}$, $tq\bar{b}$	Untagged b, jet misidentified as lepton
Drell-Yan	$Z/\gamma^* \to ee, \mu\mu$	"Fake" $E_{\mathrm{T}}^{\mathrm{miss}}$
	$Z/\gamma^* \to \tau\tau \to \ell\nu\nu\ell\nu\nu$	Real leptons and neutrinos
Other dibosons	$ZZ \to \ell\ell\nu\nu$	Real leptons and neutrinos
	$W\gamma^*, WZ \to \ell\nu\ell\ell, ZZ \to \ell\ell\ell\ell$	Unreconstructed leptons
	$W\gamma, Z\gamma$	γ reconstructed as e, unreconstructed lepton
W+jets	$Wj \to \ell\nu j$	Jet reconstructed as lepton
QCD multijet	jj	Jets reconstructed as leptons

Table 3.1: A summary of backgrounds to the $H \to WW^* \to \ell\nu\ell\nu$ signal

boson fusion, and associated production of a Higgs all lead to unique final state topologies. Figure 3.6 delineates the different signal regions used in the gluon fusion and vector boson fusion $H \to WW^*$ analyses. While there are different optimizations possible in each signal region, there are also some commonly shared selections that will be described here.

3.4.1 Event pre-selection

Before being sorted into the distinct signal regions, basic cuts are applied on the reconstructed objects in the event to select Higgs-like event candidates. First, two oppositely charged leptons are required. The p_{T} threshold on the leptons is a particularly important consideration for this signal. Because the second W produced in the decay can be off-shell, it tends to produce lower momentum leptons. Thus, being able to lower the p_{T} threshold while still maintaining a low background rate is critical. Figure 3.7 shows an example of the subleading lepton p_{T} for a VBF $H \to WW^*$ signal compared to the corresponding $t\bar{t}$ background. Note that the lepton p_{T} spectrum is considerably softer in the signal sample.

Once the leptons are selected, the last requirement for event pre-selection is the presence of neutrinos. As neutrinos cannot be detected directly in ATLAS, $E_{\mathrm{T}}^{\mathrm{miss}}$ can be used as a proxy for the combined neutrino momentum in the transverse plane. In general, it is expected that the signal should have a harder

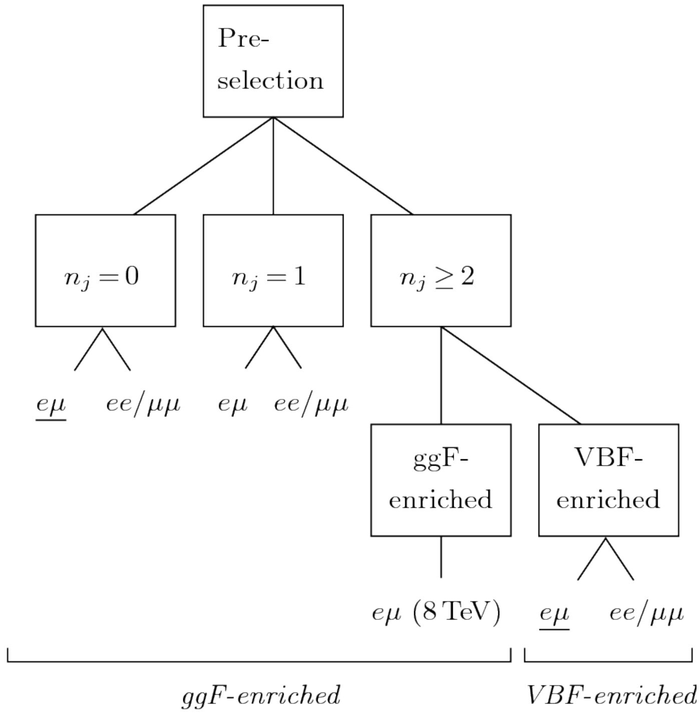

Figure 3.6: An illustration of the unique analysis signal regions [1]

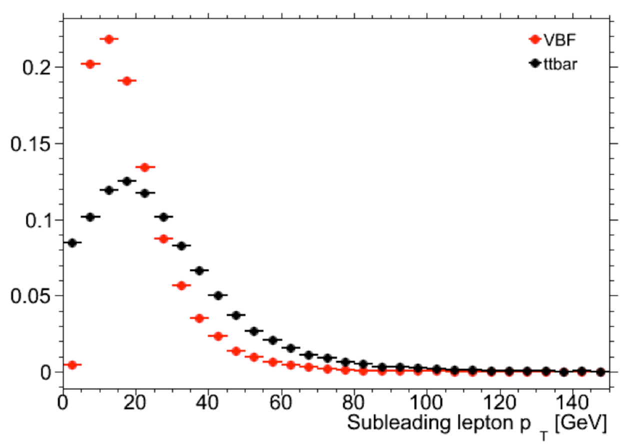

Figure 3.7: A comparison of the subleading lepton p_{T} spectrum between VBF $H \to WW^*$ production and $t\bar{t}$ background

$E_{\mathrm{T}}^{\mathrm{miss}}$ spectrum than backgrounds, especially if those backgrounds did not contain neutrinos. One additional consideration when using $E_{\mathrm{T}}^{\mathrm{miss}}$ is the fact that mis-measurements of objects in the detector can lead to imbalances in the transverse plane that are not due to real particles escaping the detector. One indicator that this is the case is that the $E_{\mathrm{T}}^{\mathrm{miss}}$ vector in the transverse plane will be pointing in the same direction as the mis-measured object. Therefore, a new variable, $E_{\mathrm{T,rel}}^{\mathrm{miss}}$, is used in the pre-selection. $E_{\mathrm{T,rel}}^{\mathrm{miss}}$ is defined in equation 3.1.

$$E_{\mathrm{T,rel}}^{\mathrm{miss}} = \begin{cases} E_{\mathrm{T}}^{\mathrm{miss}} \sin \Delta\varphi_{\mathrm{near}} & \text{if } \Delta\varphi_{\mathrm{near}} < \pi/2 \\ E_{\mathrm{T}}^{\mathrm{miss}} & \text{otherwise,} \end{cases} \tag{3.1}$$

If the closest object to the $E_{\mathrm{T}}^{\mathrm{miss}}$ vector is within $\pi/2$ radians in the transverse plane, the $E_{\mathrm{T}}^{\mathrm{miss}}$ is projected away from this object. Otherwise, the normal $E_{\mathrm{T}}^{\mathrm{miss}}$ vector is used. Figure 3.8 shows a graphical illustration of this concept.

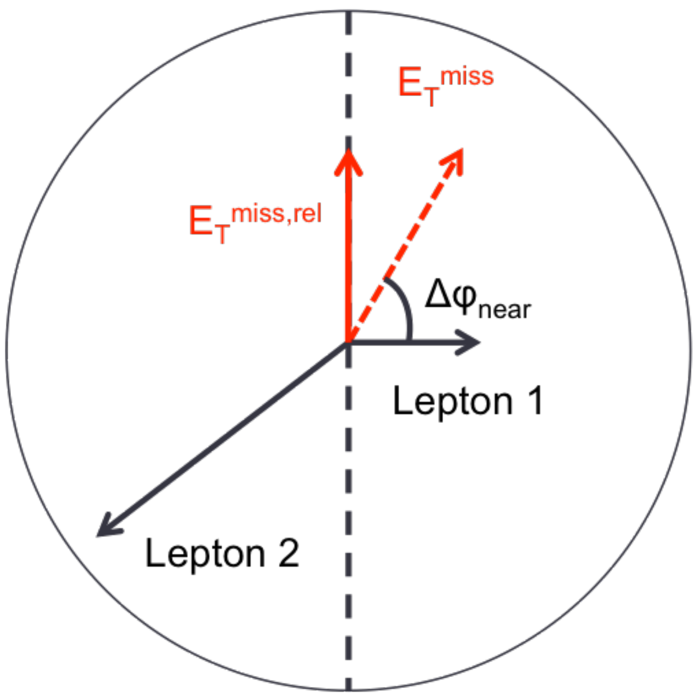

Figure 3.8: A graphical illustration of the $E_{\mathrm{T,rel}}^{\mathrm{miss}}$ calculation

Once both the lepton and $E_{\mathrm{T}}^{\mathrm{miss}}$ pre-selections are made, the analysis can be divided into different regions according to jet multiplicity.

3.4.2 Jet multiplicity

Jet multiplicity, denoted as n_j, is used to sub-divide the analysis into its distinct signal regions. The reason for this is twofold. First, different jet multiplicity bins will be more or less sensitive to different Higgs production modes. For example, the $n_j \geq 2$ region is more sensitive to VBF production because of the two hard jets produced at matrix element level. For gluon fusion production to enter this bin, two initial state radiation jets must be emitted. Second, background composition varies greatly in different bins of n_j. Figure 3.9 shows the jet multiplicity in both the different flavor and same flavor regions. It also shows the background composition in the bins of n_b. There are a few clear trends from this distribution. The first is that the Drell-Yan background dominates in the same flavor channels for $n_j \leq 1$. Second, the top background becomes a clear contributor to the total background for $n_j \geq 1$. Lastly, the SM WW production dominates in the $n_j = 0$ bin, as it is an irreducible background to $H \to WW^*$ production. Because of these distinct features, each jet multiplicity bin is treated separately.

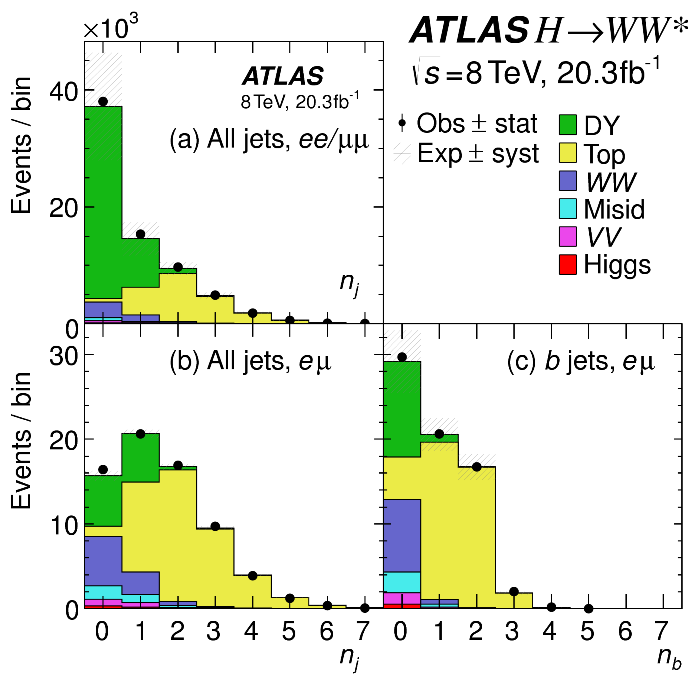

Figure 3.9: Predicted backgrounds (compared with data) as a function of n_j (a and b) and n_b (c)

3.5 Background reduction in same-flavor final states

3.6 Parameters of interest and statistical treatment

4

The discovery of the Higgs boson and the role of the $H \to WW^* \to \ell\nu\ell\nu$ channel

5

Observation of Vector Boson Fusion production of $H \to WW^* \to \ell\nu\ell\nu$

6

Combined Run 1 $H \to WW^* \to \ell\nu\ell\nu$ results

Part III

Search for Higgs pair production in the $HH \to b\bar{b}b\bar{b}$ channel in LHC Run 2 at $\sqrt{s} =$ 13 TeV

7

Search overview

8

Search for Higgs pair production in boosted final states

9

Results with Run 2 2015 dataset

Part IV

Looking ahead

10

Conclusion

We found the Higgs. Then measured it. Then used it to look for new physics. What a time to be alive!

References

[1] Collaboration, A. (2015). Observation and measurement of higgs boson decays to ww* with the atlas detector. *Phys. Rev. D*, 92(012006).

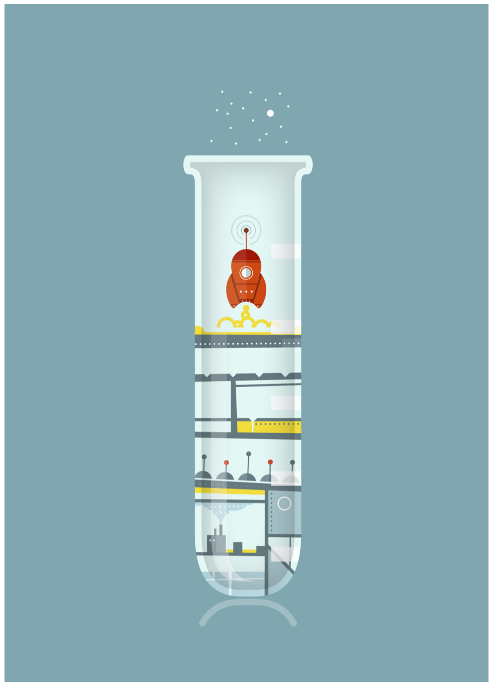

This thesis was typeset using LaTeX, originally developed by Leslie Lamport and based on Donald Knuth's TeX. The body text is set in 11 point Egenolff-Berner Garamond, a revival of Claude Garamont's humanist typeface. The above illustration, *Science Experiment 02*, was created by Ben Schlitter and released under CC BY-NC-ND 3.0. A template that can be used to format a PhD dissertation with this look & feel has been released under the permissive AGPL license, and can be found online at github.com/asm-products/Dissertate or from its lead author, Jordan Suchow, at suchow@post.harvard.edu.